Regular Article

PHYSICAL CHEMISTRY RESEARCH
Published by the
Iranian Chemical Society
www.physchemres.org
info@physchemres.org

Phys. Chem. Res., Vol. 13, No. 4, 743-754, December 2025
DOI: 10.22036/pcr.2025.510123.2665

Density Functional Theory Approach on the Mechanism of Uncatalysed Oxidation of 4-[(4-Methylphenyl) amino]-4-oxobutanoic Acid by Alkaline Potassium Permanganate

S. Shashidhar[a,b,*], Vidyavati A. Shastry[b], K. Gurushantha[c,*], K.S. Ravindra[d], V.S. Anusuya Devi[a] and P.K. Asha[a]

[a]*Department of Chemistry, New Horizon College of Engineering, Outer Ring Road, Bangalore-560103, Karnataka, India*

[b]*Department of Chemistry, Visvesvaraya Technological University, SEA College of Engineering & Technology, Bangalore-560049, Karnataka, India*

[c]*Department of Chemistry, M.S. Ramaiah Institute of Technology (Affiliated to Visvesvaraya Technological University, Belgaum), Bengaluru, Karnataka 560054, India*

[d]*Department of Chemistry, PES Institute of Technology and Management, Sagar Road, Guddada Arakere, Kotegangoor, Shivamogga-577204, Karnataka, India*

(Received 30 March 2025, Accepted 23 August 2025)

The study of 4-[(4-methyphenyl) amino]-4-oxobutanoic acid (MPOX) oxidation kinetics by alkaline $KMnO_4$ at constant 0.01 mol dm^{-3} ionic strength applied density functional theory (DFT) method using a spectrophotometric method. The manganate displayed first-order behavior, while each item of MPOX and media behaved with relation to the power of less than one. The LC-MS method was employed to determine the reaction product, while the rate constants for each step of the mechanistic pathway were calculated, and the activation parameters from the slow reaction step were determined and presented in a table. A suitable reaction mechanism along with the corresponding rate law has been developed for this reaction. The DFT method was used to analyze the HOMO-LUMO of both the starting material and the final product. Stepwise reaction processes were determined through the combination of computational results that included thermodynamic parameters, density of states analysis, electronic properties, natural bond order information, and Mulliken charge data. Fukui condensed functions for MPOX demonstrate the calculations regarding nucleophilic and electrophilic interaction and radical attack, together with the acceptor-donor bonding properties of orbital bonds. The stability and reactivity of the reactant and product are compared with various calculated electronic parameters.

Keywords: Kinetics, 4-[(4-Methyphenyl) amino]-4-oxobutanoic acid, Mechanism, Rate law, Density functional theory, Donor, Acceptor

INTRODUCTION

4-[Amino(4-methylphenyl)]4-oxobutanoic acid (MPOX), with the chemical formula of $C_{11}H_{13}NO_3$, has a structure consisting of a butanoic acid backbone with a 4-methylphenylamino group and a keto group inserted at the fourth carbon. The development of aryl-4-oxobutanoic acid amide derivatives aimed to replicate the μ-calpain inhibitory properties of chromone and quinolinone derivatives through acyclic structure modifications [1]. The application of 4-oxobutanoic acid derivatives for inflammation treatment has received patent approval [2]. The conversion of carvacrol and thymol derivatives into alkyl-4-oxobutanoate molecules led to better tyrosinase inhibitory activity [3]. Researchers have synthesized many derivatives of 4-oxobutanoic acid,

*Corresponding authors. E-mail: shashidharchem32@gmail.com; gurushanthak2016@gmail.com

and their antitumor and antibacterial properties have been studied [4,5]. Chemicals with comparable structures are frequently used in medicinal research and organic synthesis. They can be used as reference compounds in analytical investigations or as intermediates in the production of other bioactive chemicals [6].

The environmental management strategy of permanganate oxidation offers numerous advantages because it is cheap to implement and operate and exhibits diverse reactivity ranges [7]. The reactivity trends for Permanganate compounds are studied throughout various model organic compounds together with organic contaminants [8,9]. The reaction rate constants between permanganate and aromatic rings, as well as alcohols and ether groups, remained low [10,11]. Reaction sites in alkenes demonstrated the fastest rate constants among all examined organic molecules before phenol and aniline groups and benzylic carbon–hydrogen bonds [12]. The rate of permanganate reactions is affected by electrophilic substitution principles since donating electrons accelerates the reaction, but withdrawing electrons slows it down [13,14]. The oxidizing power of permanganate ions enables them to oxidize multiple types of substrates [15-18], which leads to their widespread usage in organic manufacturing processes.

Due to 4-oxobutanoic acid derivatives wide applications, the present work investigates the kinetics, mechanism, and computational analysis using density functional theory. The structure of MPOX is represented in Fig. 1.

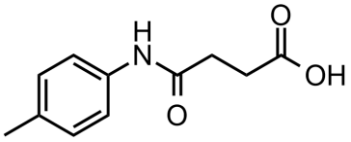

Fig. 1. Structure of 4-[(4-methylphenyl) amino]-4-oxobutanoic acid.

MATERIAL AND METHODS

Materials

Sodium Hydroxide, Potassium nitrate, Potassium Permanganate were procured from SD Fine chemicals company and were of analytical grade quality. Other chemicals, methanol and acrylonitrile, used in the studies were of analytical grade quality and were purchased from Merck. Corning glassware was utilized to make the solutions in deionized water. A 0.01 mol dm^{-3} potassium permanganate solution was prepared through the solution of salt in doubly distilled water. The solution obtained standardization through a Systronics UV-Visible spectrophotometer by assessing its absorbance at 525 nm. Additionally, Potassium nitrate, Sodium Hydroxide were made in deionized water and standardized using accepted techniques.

Kinetic Measurements

Pseudo first-order conditions applied when permanganate reacted with 4-[(4-methylphenyl) amino]-4-oxobutanoic acid in an alkaline solution maintaining a constant ionic strength of 0.01 mol dm^{-3}. A combination of thermally equilibrated solutions containing both [MnO_4^-] and [MPOX] with their required components of KNO_3 and NaOH initiated the reaction. The reaction track occurred using spectrophotometry to observe the permanganate-triggered reduction of absorbance at the 525 nm wavelength. The reaction's pseudo-first-order rate constants were determined from log[MnO_4^-] *vs.* time plots after reaching more than 80% reaction completion point [19]. The measurement of rate constants possessed a reproducibility of ±5%. The outcomes are tabulated in Table 1.

Product and Stoichiometry Analysis

Reactions with different [MnO_4^-] and [MPOX] ratios were allowed to reach equilibrium during 24 h at 25 °C with all other reactants unchanged to evaluate the reaction stoichiometry. The spectrophotometric determination proves that one mole of MPOX requires four moles of permanganate in accordance with the reaction presented in Eq. (1.1). After extraction by ether, the substances underwent desiccation before analysts performed their evaluation. LC-MS evaluation of the product indicated the establishment of 4-[(4-carboxyphenyl)amino]-4-oxobutanoic acid, which showed an M-1 peak at 236.

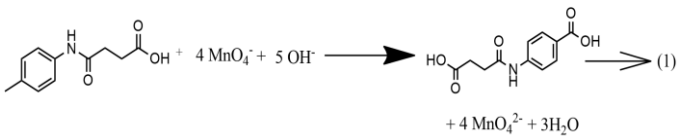

Table 1. The Influence of Varying Concentrations of [MnO_4^-], [MPOX], [NaOH], and [KNO_3] on the Oxidation Process of 4-[(4-Methylphenyl) amino]-4-oxobutanoic Acid by Alkaline $KMnO_4$, while Maintaining a Constant Ionic Strength of 0.01 mol dm^{-3} at a Temperature of 298 K

$[MnO_4^-] \times 10^{-4}$ (mol dm^{-3})	$[MPOX] \times 10^{-3}$ (mol dm^{-3})	$[NaOH] \times 10^{-2}$ (mol dm^{-3})	$[KNO_3] \times 10^{-2}$ (mol dm^{-3})	$k_{obs} \times 10^{-2}$ (s^{-1}) Experimental	$k_{cal} \times 10^{-2}$ (s^{-1}) Calculated
0.5	2.5	1.0	1.0	2.36	2.42
1.5	2.5	1.0	1.0	2.38	2.42
2.5	2.5	1.0	1.0	2.39	2.42
3.5	2.5	1.0	1.0	2.38	2.42
4.5	2.5	1.0	1.0	2.41	2.42
2.5	0.5	1.0	1.0	0.53	0.48
2.5	1.5	1.0	1.0	1.21	1.32
2.5	2.5	1.0.	1.0	2.39	2.42
2.5	3.5	1.0	1.0	3.73	3.52
2.5	4.5	1.0	1.0	5.94	4.64
2.5	2.5	0.25	1.0	1.35	1.43
2.5	2.5	0.5	1.0	1.85	1.78
2.5	2.5	1.0	1.0	2.39	2.4
2.5	2.5	2.0	1.0	2.72	2.64
2.5	2.5	3.0	1.0	3.12	2.94
2.5	2.5	1.0	0.25	1.32	2.42
2.5	2.5	1.0	0.5	1.35	2.42
2.5	2.5	1.0	1.0	1.39	2.42
2.5	2.5	1.0	2.0	1.28	2.42
2.5	2.5	1.0	3.0	1.19	2.42

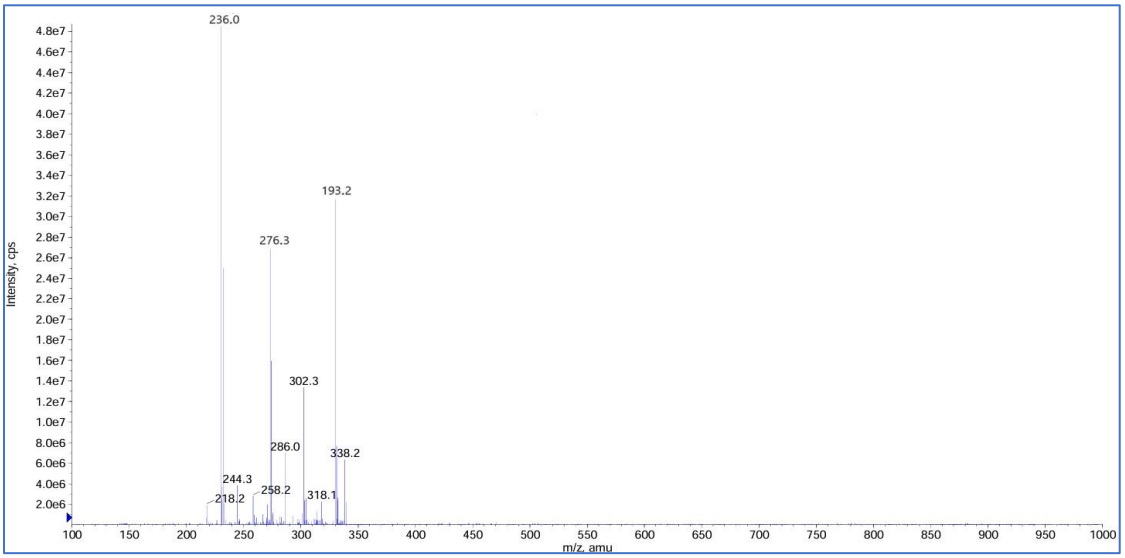

Fig. 2. LC-MS revealing the oxidation product 4-[(4-carboxyphenyl)amino]-4-oxobutanoic acid in a basic environment.

Determining Reaction Orders

A set of experiments analyzed influence of permanganate by changing concentrations from 0.5 × 10^{-4} to 4.5 × 10^{-3} mol dm^{-3}, throughout which MPOX, KNO_3, and NaOH stayed constant. The reaction's first-order behavior regarding oxidant becomes readily evident from a straight line established by plotting logk values against time to 85% of reaction completion.

The impact of MPOX on the reaction rate was investigated by varying its concentration from 0.5×10^{-3} to 4.5×10^{-3} mol dm^{-3}, while keeping the concentrations of $KMnO_4$, KNO_3, and NaOH constant. A graph depicting logk against log[MPOX] suggests a first-order relationship, as shown in Fig. 3.

The influence of sodium hydroxide on the rate's reaction was examined by altering its concentration from 0.25×10^{-2} to 3.0×10^{-2} mol dm^{-3} while maintaining constant amounts of MPOX, $KMnO_4$, and KNO_3. The values of rate constants exhibit an increase with a rise in [NaOH], indicating a dependency characteristic of a fractional order of 0.32.

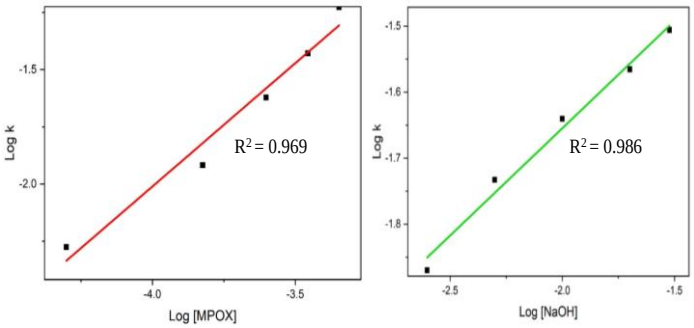

Fig. 3. Order with respect to 4-[(4-methylphenyl) amino]-4-oxobutanoic acid and NaOH on oxidation of MPOX.

Influence of Ionic Strength, Dielectric Constant of Medium, and Free Radical Intervention

The influence of ionic effect was examined by adjusting the concentration of KNO_3 from 0.25×10^{-2} to 3.0×10^{-2} mol dm^{-3}, while maintaining the concentrations of all other reactants constant. The investigation revealed that there is no notable impact on the rate. The influence of the dielectric constant of the medium on the oxidation rate of MPOX was examined [20] through the incremental addition of varying volumes of methanol to the solution mixture, while maintaining a constant concentration of the other reactants, showing no effect on the initial rate.

Free radicals' involvement in MPOX oxidation by Permanganate was studied through the introduction of acrylonitrile, followed by methyl alcohol dilution according to [21]. The sequence leads to no precipitate formation, which indicates that the pathway contains no radical mechanism. The progress of the reaction occurs through ionic components.

Effect of Temperature. The evaluation of reaction rates occurred under different temperatures when all chemical concentrations and other conditions remained stable [22]. Temperature elevation directly affected the reaction rate positively. The experimental activation energy E_a, alongside the frequency factor log A, can be obtained from the linear relationship between logk and 1/T. The results featuring parameters $\Delta H^{\#}$, $\Delta S^{\#}$, and $\Delta G^{\#}$ obtained from the Eyring equation analysis were displayed in a table format.

Table 2. Temperature Effect on rate Constant and Calculated Activation Parameters of Oxidation on MPOX

Temperature (K)	$k \times 10^{-2}$ (s^{-1})	Activation parameters	Values
298	2.39	Ea (KJ mol^{-1})	47.03
303	2.82	$\Delta H^{\#}$ (KJ mol^{-1})	44.55
308	4.15	$\Delta S^{\#}$ (KJ mol^{-1})	-186.98
313	5.80	$\Delta G^{\#}$ (KJ/K/mol)	100.3
318	7.42	logA	6.6

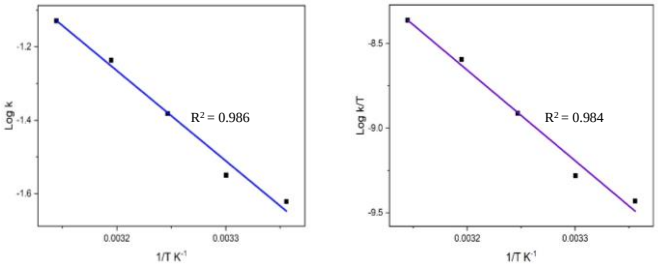

Fig. 4. a) Arrhenius b) Eyring plot showing temperature effect for the oxidation Process.

Reaction Mechanism

The speed of enolization exceeds the rate of oxidation by approximately 12.0-15.0 times in this research, and the enolization occurs through the enol form of the keto group in 4-[amino(4-methylphenyl)]4-oxobutanoic acid [23]. Enol formation serves as a fast reaction that does not determine the rate of reaction; therefore will be considered as the forward step. Scheme 2 displays the proposed mechanism for this reaction.

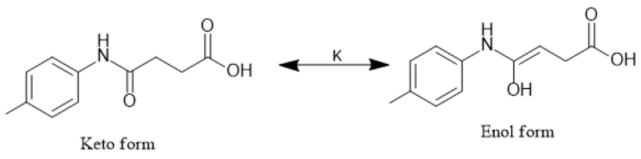

Fig. 5. Keto and enol forms of 4-[amino(4-methylphenyl)]4-oxobutanoic acid.

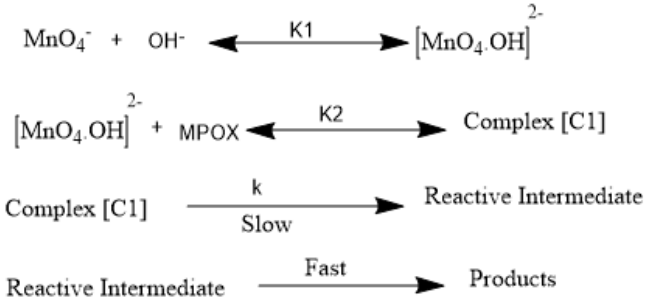

Scheme 1. Schematic representation of oxidation of 4-[amino(4-methylphenyl)]4-oxobutanoic acid by alkaline permanganate

Reactive species of permanganate ion in alkaline medium $[MnO_4.OH]^{2-}$ formed in the first equilibrium step of the mechanism. The formed species forms a complex (C1), which further abstracts an electron from MPOX to form a cation form of the compound. This intermediate, in subsequent rapid steps, combines with the permanganate ion complex in the basic medium to yield the final product. The rate law for the above mechanism is deduced and provided in Scheme 7.3.

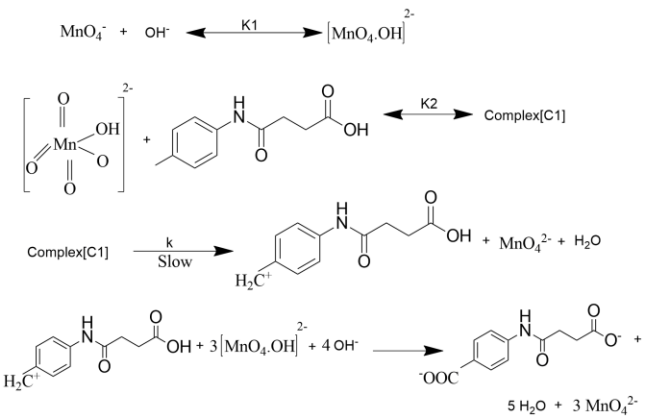

Scheme 2. Mechanism of oxidation of 4-[amino(4-methylphenyl)]4-oxobutanoic acid by alkaline permanganate

$$\text{Rate} = \frac{-d[MnO_4^-]}{dt} = k[C1]$$

$$= k K_2 [MnO_4OH]^{2-} [MPOX]$$

$$= k K1 K_2 [MnO_4^-] [OH]^- [MPOX] \longrightarrow (2)$$

$$[MnO_4^-]_t = [MnO_4^-]_f + K_1[MnO_4^-]_f [OH]_f^-$$

$$[MnO_4^-]_t = [MnO_4^-]_f (1 + K_1 [OH]_f^-)$$

$$[MnO_4^-]_f = \frac{[MnO_4^-]_t}{1+K_1 [OH]_f^-} \longrightarrow (3)$$

Where 't' represents total and 'f' represents formation

$$[MPOX]_t = [MPOX]_f + K1 K_2 [MPOX]_f [MnO_4^-]_f [OH]_f^-$$

$$[MPOX]_t = [MPOX]_f (1+K1 K_2 [MnO_4^-]_f [OH]_f^-)$$

$$[MPOX]_f = \frac{[MPOX]_t}{1+K1 K_2 [MnO_4^-]_f [OH]_f^-} \longrightarrow (4)$$

Similarly

$$[OH]_t^- = [OH]_f^- + K_1[MnO_4^-]_f [OH]_f^-$$

$$= [OH]_f^- (1+K1 [MnO_4^-]_f)$$

$$[OH]_f^- = \frac{[OH]_t^-}{(1+K1 [MnO_4^-]_f)} \longrightarrow (5)$$

On substituting $[OH^-]_f$, $[MPOX]_f$ and $[MnO_4^-]_f$ in equation (2)

$$\text{Rate} = \frac{k K1 K_2 [MnO_4^-] [OH]^- [MPOX]}{(1+K_1 [OH]_f^-)(1+K1 K_2 [MnO_4^-]_f [OH]_f^-) (1+K1 [MnO_4^-]_f)}$$

On negelectiong the concentration of Permanganate in denominator and rearraging the equation

$$\frac{\text{Rate}}{[MnO_4^-]} = k_{obs} = \frac{k K1 K_2 [MPOX][OH]^-}{1+K_1[OH]^-} \longrightarrow (6)$$

$$\frac{1}{k_{obs}} = \frac{1}{k K1 K_2 [MPOX][OH]^-} + \frac{1}{k K_2 [MPOX]} \longrightarrow (7)$$

Scheme 3. Rate law derivation for oxidation of 4-[amino(4-methylphenyl)]4-oxobutanoic acid by alkaline permanganate

COMPUTATION DETAILS

Quantum calculation was carried out using density functional theory, within Becke-Lee-Parr hybrid exchange-correlation three-parameter functional (B3LYP) and using the standard 6-311G+(d,p) basis set[24]. An optimized structure was used to compute the full geometry optimization and the vibrational frequencies up to B3LYP/6-311G+(d,p) level. Details of thermodynamic data and electronic parameters were retrieved from the frequency optimized log file using GaussView, and calculations of different parameters were performed using well-acknowledged methods. Gaussian 09 software has been used to extract a HOMO-LUMO image, a molecular energy potential map (MESP). GaussSum software was used to obtain the density of state (DOS) spectra of the product and reactant. Fukui functions, local philicities data are extracted from UCA-FUKUI software using the frontier molecular orbital (FMO) approximation method.

COMPUTATION CALCULATION OF MPOX AND ITS PRODUCT

Density functional theory is a powerful tool to understand the reaction mechanism pathway based on its charge distribution, electronic structure, bonding, and reactive site. Becke, 3-parameter, Lee-Yang-Parr [25,26], a hybrid functional tool, is widely used method to analyse a variety of organic molecular structures. To understand the chemical and electrical nature of MPOX and its oxidation product, the Gaussian 09 program was utilized. The thermodynamic data obtained from the frequency optimized structures are given in Table 3.

The electrical energy data is utilised to determine the stability of molecules [27], in the above data even though 4-[(4-carboxyphenyl)amino]-4-oxobutanoic acid is lowered in -[(4-methylphenyl) amino]-4-oxobutanoic acid, the stability of product may due to more decrease in thermal energy and is also supported by more degree of randomness due to more entropy. This extra stability of the product is further supported by lesser thermal correlation to free energy.

HOMO (Highest Occupied Molecular Orbital) and LUMO (Lowest Unoccupied Molecular Orbital) give valuable information on the stability and reactivity of molecules. By knowing the HOMO-LUMO energy gap, one can ascertain its characteristics [28,29]. The HOMO-LUMO can be calculated as

$$\Delta E = E_{\text{LUMO}} - E_{\text{HOMO}}$$

In our study, the observed HOMO-LUMO energy gap of MPOX and its products were calculated as 5.71 eV and 4.92 eV, which can explain the oxidation product 4-[(4-carboxyphenyl)amino]-4-oxobutanoic acid still may further degrade into simple parts due to its reactivity. A small HOMO-LUMO energy gap indicates it can easily accept or donate electrons [30].

The molecule electrostatic potential (MESP) is the surface diagram of the molecules by which the nature of the molecule with electrophilic or nucleophilic attacking sites can be predicted [31]. The red region shows highly negative potential, these are the nucleophilic sites which can readily attached by the electrophile.

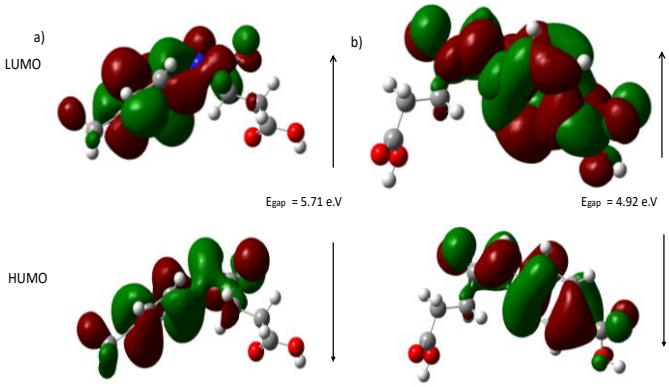

Fig. 5. HOMO-LUMO of a) -[(4-methylphenyl) amino]-4-oxobutanoic acid and b) 4-[(4-carboxyphenyl) amino]-4-oxobutanoic acid with HOMO-LUMO energy gap.

Table 3. Thermodynamic Data Generated from DFT Using the B3LYP/6-311G++(d,p) Method without Solvation

Thermodynamic data	4-Oxo-4(p-tolylamino) butanoic acid	4-[(4-Carboxyphenyl)amino]-4-oxobutanoic acid
Electronic energy (EE) (eV)	-19248.67	-23309.83
Zero-point energy correction (eV)	6.13	5.80
Thermal correction to energy (eV)	6.53	6.23
Thermal correction to enthalpy (eV)	6.56	6.26
Thermal correction to Free energy (eV)	4.88	4.53
EE + Zero-point energy (eV)	-19242.54	-23304.02
E (Thermal) kJ mol^{-1}	631.02	602.22
Heat capacity (Cv) J $mol^{-1}K^{-1}$	226.86	243.51
Entropy (S) J mol^{-1} K^{-1}	542.96	561.32

Blue regions have highly positive potential sites, as they are electrophilic sites that readily react with nucleophiles. Green or yellow regions are neutral potential regions that have intermediate polarity, generally non-reactive in nature. Figure 6 a) shows blue region on the methyl group, which is more susceptible to attack by the anionic nucleophile $[MnO_4.OH]^{2-}$ generated by Permanganate ion.

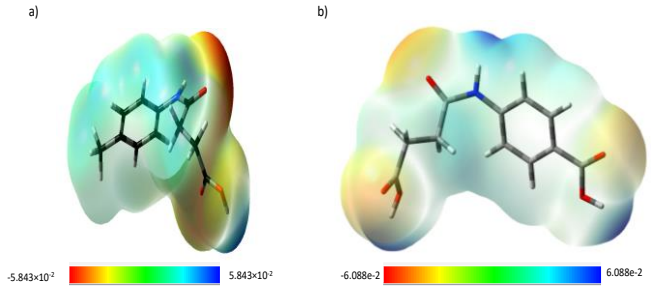

Fig. 6. Electrostatic potential map with total density state of a) -[(4-methylphenyl) amino]-4-oxobutanoic acid and b) 4-[(4-carboxyphenyl)amino]-4-oxobutanoic acid with HOMO-LUMO energy gap.

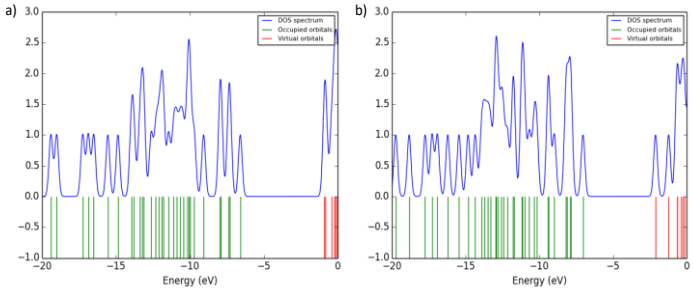

Fig. 7. Density of state (DOS) spectrum of a) -[(4-methylphenyl) amino]-4-oxobutanoic acid and b) 4-[(4-carboxyphenyl)amino]-4-oxobutanoic acid.

The generated DOS spectrum energy gap estimation of 4-[(4-carboxyphenyl)amino]-4-oxobutanoic acid (Fig. 7 b) from the GaussSum program shows larger energy gap, hence it requires more energy to promote an electron from the occupied state to the unoccupied state. It shows reasonable stability and less reactivity compared to the reactant MPOX.

Fukui condensed functions were widely applied to study the reactivity indexes [32,33,34] Fukui condensed functions (f^+, f^-, f^0) obtained based on Frontier molecular orbital method provides valuable information regarding active sites for electrophilic, nucleophilic and radical attack of reactant MPOX (Table 4), according to this computational study potential electrophilic attacking sites are atom 25 (carbon) and 26 (oxygen) which has a value of 0.62 and 0.35. The potential nucleophilic site atom 18 (oxygen) with the highest value of 0.97, the dominant radical attack sites in MPOX are atom 18 (oxygen), 25 (carbon), and 26 (oxygen) with high values of 0.48, 0.31, 0.17, respectively, as shown in Fig. 8.

The Mulliken charges are computed employing Natural Bond Order analysis, which shows the carbon atom of the methyl group attached to the aromatic ring has a more negative charge value of 0.66 e, indicating a more electronegative nature, and the hydrogen attached to it has lower occupancy of electrons and is acidic in nature [35]. This explains the stability of the cationic form of MPOX formed during our proposed mechanism.

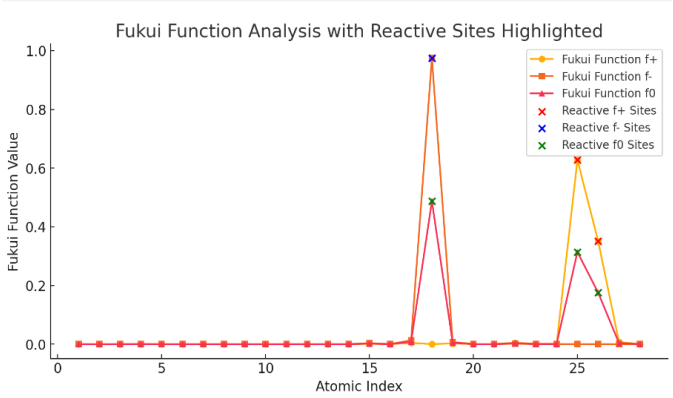

Fig. 8. Condensed Fukui analysis for electrophilic, nucleophilic, and radical attack sites of MPOX.

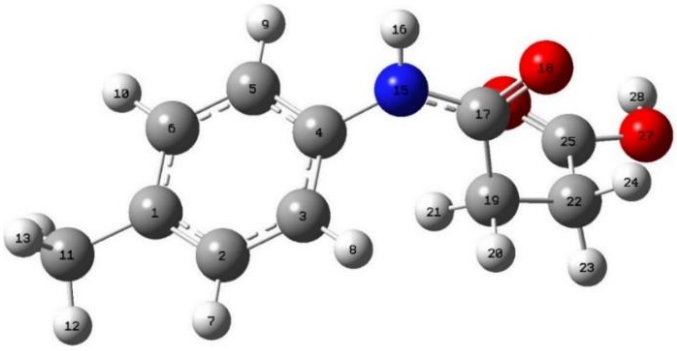

Fig. 9. Geometry optimized structure showing atomic labels of MPOX for NBO analysis.

Table 4. Fukui Functions, Local Philicities, and Mulliken Charges Computed for MPOX from DFT Using NBO Analysis

Atom label	atom	Fukui condensed function f+	Fukui condensed function f-	Fukui condensed function (f, raricalary attack)	Local philicities w+ (eV)	Local philicities w- (eV)	Mulliken charges
1	C	0	0	0	0	0	0.45
2	C	0	0	0	0	0	-0.28
3	C	0.0003	0	0.0001	0.0002	0	0.25
4	C	0.0003	0.0003	0.0003	0.0002	0.0002	-0.49
5	C	0.0002	0	0.0001	0.0001	0	-0.13
6	C	0	0	0	0	0	-0.27
7	H	0	0	0	0	0	0.18
8	H	0	0	0	0	0	0.18
9	H	0	0	0	0	0	0.18
10	H	0	0	0	0	0	0.17
11	C	0	0	0	0	0	-0.67
12	H	0	0	0	0	0	0.15
13	H	0	0	0	0	0	0.17
14	H	0	0	0	0	0	0.14
15	N	0.0012	0.0026	0.0019	0.0009	0.0018	-0.08
16	H	0	0.0001	0	0	0	0.30
17	C	0.0039	0.013	0.0084	0.0028	0.0092	-0.17
18	O	0.0001	0.9746	0.4874	0.0001	0.6868	-0.29
19	C	0.0023	0.0071	0.0047	0.0016	0.005	0.02
20	H	0	0.0002	0.0001	0	0.0002	0.16
21	H	0.0001	0	0.0001	0.0001	0	0.22
22	C	0.0046	0.0016	0.0031	0.0032	0.0012	-0.51
23	H	0.001	0.0001	0.0005	0.0007	0	0.19
24	H	0.0008	0.0002	0.0005	0.0005	0.0001	0.25
25	C	0.6275	0.0002	0.3139	0.4422	0.0001	-0.01
26	O	0.3504	0	0.1752	0.2469	0	-0.26
27	O	0.0072	0	0.0036	0.0051	0	-0.16
28	H	0	0	0	0	0	0.28

Further NBO analysis for Donor acceptor orbital interaction [36,37] on C_{11} carbon atom shows that C_{11}-H_{12}, and C_{11}-H_{13} bonding orbitals (Table 6) have very good stabilization energy with antibonding orbitals of C_1-C_6 and C_1-C_2, which indicates the stronger donor-acceptor interaction. These interactions are also supported by high Fock Matrix element F(i,j) values showing the hyperconjugation effect of hydrogens present in the methyl group.

Stability Comparison of [(4-Methylphenyl) amino]-4-Oxobutanoic Acid and 4-[(4-Carboxyphenyl)amino]-4-oxobutanoic Acid

Ionization Potential, Electron Affinity, Electronegativity, Hardness, and HOMO-LUMO energy gap provide valuable information regarding the stability and reactivity of compounds [38,39,40]. The [(4-methylphenyl) amino]-4-oxobutanoic acid has a larger HOMO-LUMO energy gap of 5.68 eV (Table 6) indicating more stability compared to its

Table 5. NBO Analysis for the Acceptor Donor Site, along with Stabilization Energy

Bonding donor orbital	Acceptor orbital	Acceptor orbital type	Stabilization energy (kcal mol^{-1})	E(j) - E(i) (eV)	F(i,j) (a.u.)
C_{11} - H_{12}	C_1	RY*	0.51	1.73	0.026
C_{11} - H_{12}	C_1 - C_2	BD*	0.81	0.54	0.021
C_{11} - H_{12}	C_1 - C_6	BD*	3.89	1.08	0.058
C_{11} - H_{13}	C_1	RY*	0.94	1.22	0.03
C_{11} - H_{13}	C_1 - C_2	BD*	0.6	1.08	0.023
C_{11} - H_{13}	C_1 - C_2	BD*	4.5	0.54	0.048
C_{11} - H_{14}	C_1 - C_2	BD*	3.76	1.08	0.057
C_{11} - H_{14}	C_1 - C_2	BD*	1.17	0.54	0.025

Table 6. Electronic Parameters of Reactant and Product in the Gas Phase

Molecular Parameters (eV)	[(4-Methylphenyl) amino]-4-oxobutanoic acid	4-[(4-Carboxyphenyl)amino]-4-oxobutanoic acid
EHOMO (eV)	-6.57	-7.03
ELUMO (eV)	-0.89	-2.11
Ionization Potential (IP)	8.27	8.74
Electron Affinity (EA)	-0.25	0.49
HOMO-LUMO Energy gap (eV)	5.69	4.93
Electronegativity (χ)	4.02	4.62
Chemical Potential (μ)	-4.26	-4.13
Chemical Hardness (η)	4.26	4.13
Chemical Softness (σ)	0.24	0.24
Electrophilicity Index (ω)	2.13	2.06
Nucleophilicity index (N)	2.53	2.08
Electron Donor Power (ώ+)	4.43	5.4
Electron Acceptor Power (ώ)	0.41	0.79

oxidation product with energy gap of 4.93 eV indicating the product 4-[(4-carboxyphenyl)amino]-4-oxobutanoic acid may susceptible for more interactions, but higher value of ionization potential (8,74 eV) making it more resistant to oxidation compared to reactant. A higher electron affinity of 0.49 eV, the product shows more reactiveness towards electron-donating species, more electronegative nature of the product indicates its stability in polar environments. The reactant MPOX with less chemical potential suggests its instability in our experimental conditions.

CONCLUSIONS

The methodology of DFT was utilised to study the oxidation of 4-[(4-methylphenyl) amino]-4-oxobutanoic acid, utilizing alkaline potassium permanganate. The reaction yielded a product identified as 4-[(4-carboxyphenyl) amino]-4-oxobutanoic acid. The geometric configurations of both reactants and products are meticulously optimized utilizing the Gaussian 09 program, employing the B3LYP/6-311 G++(d,p) basis set method. The diverse energy parameters are studied for both the reactant and product, while the likely structure of the formed complex is anticipated using the DFT method. The reaction order concerning MPOX, permanganate, and NaOH is established, and the influence of ionic strength and dielectric constants is examined. A suitable scheme, mechanism, and rate law have been established based on the experimental data. The parameters for activation were meticulously calculated and subsequently organized into a table.

Computational thermodynamic parameters were analysed for the reactant and product. HOMO-LUMO of the reactant are compared for the stability, along with molecular electrostatic potential map, density of states, Fukui condensed functions were utilized to determine electrophilic, nucleophilic, and radical attack site of the reactant. The hyperconjugation effect studied using natural bond order analysis for donor-acceptor sites, Mulliken charges on atoms further support our proposed mechanism. Various electronic parameters were analyzed for the stability of the reactant and product.

REFERENCES

[1] Yong, Z.; Seo Yoon, J.; Changbae, J.; Nam Doo, K.; Ping, G.; Yong Sup, L., Design and synthesis of 4-aryl-4-oxobutanoic acid amides as calpain inhibitors. *Bioorg. Med. Chem. Lett*. **2009**, *19*(2), 502-507, DOI: 10.1016/j.bmcl.2008.11.030.

[2] Moinet, G.; Marais, D.; Maizeray, P., *Use of 4-oxobutanoic acid derivatives in the treatment of inflammation.* **2004**. *European Patent Office*. EP1450780A1.

[3] Brotzman, N.; Xu, Y.; Graybill, A.; Cocolas, A.; Ressler, A.; Seeram, N. P.; Ma, H.; Henry, G. E., Synthesis and tyrosinase inhibitory activities of 4-oxobutanoate derivatives of carvacrol and thymol. *Bioinorganic. Med. Chem. Lett*, **2019**, *29*(1), 56-58. DOI: 10.1016/ j.bmcl.2018.11.013.

[4] Yang, J.; Liang, G. P.; Liu, X. L., Synthesis and antitumor activities of 4-(1H-indol-1-yl)-4-oxobutanoic acid spliced podophyllotoxin derivatives. *Synth. Commun*. **2023**, *53*(3), 262-273. DOI: 10.1080/ 00397911.2023.2164863.

[5] Sana, A.; Khan, S.; Zaidi, J.; Ambreen, N.; Khan, K.; Perveen, S., Syntheses and antimicrobial activities of amide derivatives of 4-[(2-isopropyl-5-methylcyclohexyl)oxo]-4-oxobutanoic acid. *Nat.Sci*. **2011**, *3*, 855-861. DOI: 10.4236/ns.2011.310110.

[6] Muñoz-Nuñez, C.; Cuervo-Rodríguez, R.; Echeverría, C.; Fernández-García, M.; Muñoz-Bonilla, A., Synthesis and characterization of thiazolium chitosan derivative with enhanced antimicrobial properties and its use as component of chitosan based films. *Carbohydr. Polym*. **2023**, *302*, 120438. DOI: 10.1016/ j.carbpol.2022.120438.

[7] Juliana, R. L.; Adaline, K.; Allison, A. M., Permanganate Oxidation of Organic Contaminants and Model Compounds. *Environ. Sci. Technol*. **2022**, *56*(8), 4728-4748. DOI: 10.1021/acs.est.1c03621.

[8] Mengfan, L.; Heng, Z.; Jianhua, G.; Jia, Z.; Can, F.; Jialong, Y.; Chang, X.; Ye, D.; Yang, L.; Chuan-Shu, H.; Bo, L., Proton vs Electron: The Dual Role of Redox-Inactive Metal Ions in Permanganate Oxidation Kinetics, *Environ. Sci. Technol*. **2024**, *58*(40), 18041-18051, DOI: 10.1021/acs.est.4c06557.

[9] Sean, T. M.; David, P. W.; Nigel, J. D. G., Analytical quantification of aqueous permanganate: Direct and indirect spectrophotometric determination for water treatment processes. *Chemosphere*. **2020**, *251*, 126626.o. DOI: 10.1016/j.chemosphere.2020.126626.

[10] Du, H.; Lo, P. K.; Hu, Z.; Liang, H.; Lau, K. C.; Wang, Y. N.; Lam, W. W. Y.; Lau, T. C., Lewis acid-activated oxidation of alcohols by permanganate. *Chem. Commun.* **2011**, *47*, 7143-7145. 10.1039/C1CC12024G.

[11] John, H. T., Oxidation of Alkynyl Ethers with Potassium Permanganate. A New Acyl Anion Equivalent for the Preparation of. alpha. -Keto Esters. *J. Org. Chem.* **1995**, *60*(19), 6221-6223. DOI: 10.1021/ jo00124a049

[12] Kenneth, B. W.; Yi-gui, W.; Stepan, S.; Carol, D.; Gary, T., Permanganate Oxidation of Alkenes. Substituent and Solvent Effects. Difficulties with MP2 Calculations, *J. Am. Chem. Soc.* **2006**, *9*, 128, 35. DOI: 10.1021/ ja0630184.

[13] Basheer, K.; Joseph, J.; Nair, T., Kinetics of the Oxidation of Benzhydrols with Permanganate under Phase Transfer Catalysis in Organic Solvents, *Mod. Res. Cat.* **2013**, *2*, 35-38. DOI: 10.4236/mrc.2013.22005.

[14] Thomas, S.; Markus, B., Density Functional Theory Study on the Initial Step of the Permanganate Oxidation of Substituted Alkynes. *J. Phys. Chem. A.* **2004**, *108*(20), 4455-4458. DOI: 10.1021/jp0310652.

[15] Shashidhar, S.; Vidyavati, A. S.; Sampath, C.; Hazem, E.; Dalal, Z. H.; Anusuya, D.; Gurushantha, K.; Asha, P. K., A Spectroscopic Approach on Permanganate Oxidation of 1-[(4Chlorophenyl)methyl] piperidin-4-amine in Presence of Ruthenium(III) Catalyst with DFT

Analysis on Reaction Mechanism Pathway. *Asian J. Chem.* **2023**, *35*(12), 3005-3012. DOI: 10.14233/ajchem.2023.30577.

[16] Ishaq, A.Z., Kinetics and Mechanism of Oxidation of Nicotine by Permanganate Ion in Acid Perchlorate Solutions, *Int. J. Chem.* **2010**, *2*, 1-8. DOI: 10.5539/ijc.v2n2p193.

[17] Azmat, R.; Naz, R.; Qamar, N.; Malik, I., Kinetics and mechanisms of oxidation of d-fructose and d-lactose by permanganate ion in an acidic medium. Natural science, **2012**, *4*, 466-478. DOI:10.4236/ns.2012.47063.

[18] Ravindra, K. S.; Vidyavati, A. S.; Shashidhar, S.; Kumar, M., Comparative Kinetic Study of Palladium(II) catalyzed and Uncatalysed oxidation of Ambroxol Hydrochloride with Potassium Permanganate in an aqueous Alkanine Medium: A Mechanistic Approach. *Phys. Chem. Res.* **2023**, *11*(4), 865-875. DOI: 10.22036/pcr.2022.361486.2191

[19] Dinesh, C. B.; Raviraj, M. K.; Sharanappa, T. N., Kinetics and mechanistic study of the ruthenium(III) catalyzed oxidative deamination and decarboxylation of L-valine by alkaline permanganate. *Can. J. Chem*. **2001**, *79*, 1926-1933. DOI:10.1139/v01-17.

[20] Ankita, J.; Gajala, T.; Vijay, D., Kinetics and mechanism of permanganate oxidation of nalidixic acid in aqueous alkaline medium, *J. Appl. Pharm. Sci.* **2017**, *7*(01), 135-143. DOI: 10.7324/JAPS.2017.70118.

[21] Khan, S. R.; Ashfaq, M.; Mubashir, S. M., Oxidation kinetics of crystal violet by potassium permanganate in acidic medium. *Russ. J. Phys. Chem.* **2016**, *90*, 955-961. DOI: 10.1134/S0036024416050265.

[22] Ferrari, E.; Saladini, M.; Pignedoli, F.; Spagnolo, F.; Benassi, R., Solvent effect on keto-enol tautomerism in a new β-diketone: a comparison between experimental data and different theoretical approaches, *New. J. Chem*. **2011**, *12*, 1144-0546. DOI:10.1039/C1NJ20576E.

[23] Becke, A. D., Density-functional thermochemistry. III. The role of exact exchange. *J. Chem. Phys.* **1993**, *98*(7), 5648-5652. DOI: 10.1063/1.464913.

[24] Ram, K. A.; Senthamil, S. C.; Selvaraj, S.; Sheeja, M. G. P.; Jayaprakash, P., *In Silico* Studies on the Molecular Geometry, FMO, Mulliken Charges, MESP, ADME and Molecular Docking Prediction of Pyrogallol Carboxaldehydes as Potential Anti-tumour Agents, *Phys. Chem. Res.* **2024**, *12*(2), 305-320. DOI: 10.22036/PCR.2023.402835.2359.

[25] Sarvesh, K. P., Computational Study on the Structure, Stability, and Electronic Feature Analyses of Trapped Halocarbons inside a Novel Bispyrazole Organic Molecular Cage. *ACS Omega*, **2021**, *6*(17), 11711-11728. DOI: 10.1021/acsomega.1c01019.

[26] Lachi, M.; Cheriet, M.; Djadi, N., Exploring the Interactions of Natural Flavonoids with COX-2: Insights from Molecular Docking, DFT Analysis, and ADME Calculations, *Phys. Chem. Res.* **2024**, *12*(3), 675-691. DOI: 10.22036/pcr.2023.426148.2451.

[27] Miar Marzieh, A.; Pourshamsian, K.; Oliaey, A.; Hatamjafari, F., Theoretical investigations on the HOMO-LUMO gap and global reactivity descriptor studies, natural bond orbital, and nucleus-independent chemical shifts analyses of 3-phenylbenzo [d]thiazole-2(3H)-imine and its para -substituted derivatives: Solvent and substituent effects. *J. Chem. Res.* **2021**, *45*, 174751982093209. DOI:10.1177/1747519820932091.

[28] Per, S.; Peter. P., Use of the electrostatic potential at the molecular surface to interpret and predict nucleophilic processes, *J. Phys. Chem*. **1990**, *94*(10), 3959-3961. DOI: 10.1021/j100373a017.

[29] Supriyo, S.; Bhuwan, C. J.; Vijay, J.; Archana, N. S., Computational Investigation of Geniposidic Acid as an Anticancer Agent Using Molecular Docking, Molecular Dynamic Simulation, DFT Calculation, and OSIRIS Molinspiration Profiling, *Phys. Chem. Res.* **2023**, *11*, 4, 801-823, DOI: 10.22036/pcr.2022.359603.2177.

[30] Farhan, L. M.; Saha, S.; Abe, K. S. M., Quantum Computational, Molecular Docking, Dynamics, PASS, and ADMET Analyses of Methyl α-D-Glucopyranoside Derivatives, *Phys. Chem. Res.* **2025**, *13*(2), 381-400. DOI: 10.22036/pcr.2025.491267.2601.

[31] Mcphedran, R.; Botten, L.; McOrist, J.; Asatryan, A. A.; Sterke, C.; Nicorovici, N. A., Density of states functions for photonic crystals. *Phys. Rev. E*, **2004**, *69*, 016609. DOI: 10.1103/PhysRevE.69.016609.

[32] Nicolás, F. B.; Javiera, C.; Francisco, M.; Wilver, A. M.; Tatiana, G.; Mònica, C.; Carlos C., Fukui Function and Fukui Potential for Solid-State Chemistry: Application to Surface Reactivity, *J. Chem. Theory. Comput.* **2025**, *21*(6), 3187-3203,

DOI: 10.1021/acs.jctc.5c00086.

[33] Pucci, R.; Angilella, G. G. N., Density functional theory, chemical reactivity, and the Fukui functions. *Found Chem*, **2022**, *24*, 59-71 DOI: 10.1007/s10698-022-09416-z.

[34] Echegaray, E.; Cárdenas, C.; Rabi, S.; Rabi, N.; Lee, S.; Zadeh, F. H.; Toro-Labbe, A.; Anderson, J. S.; Ayers, P. W., In pursuit of negative Fukui functions: examples where the highest occupied molecular orbital fails to dominate the chemical reactivity. *J. Mol. Model*, **2013**, *19*(7), 2779-2783. DOI:10.1007/s00894-012-1637-3.

[35] Gómez-Jeria, J., An empirical way to correct some drawbacks of mulliken population analysis. *J. Chil. Chem. Soc.* **2009**, *54*, 289. 10.4067/S0717-97072009000400036.

[36] Bauzá, A.; Frontera, A., On the Importance of Nonbonding Donor-Acceptor Interactions Involving PO_2. Radicals: An *ab Initio* Study. *Chem. Phys. Chem*. **2017**, *18*, 2191. DOI: 10.1002/cphc.201700399.

[37] Halim, S. A.; El-Meligy, A. B.; El-Nahas, A. M., DFT study, and natural bond orbital (NBO) population analysis of 2-(2-Hydroxyphenyl)-1-azaazulene tautomers and their mercapto analouges. *Sci. Rep.,* **2024**, *14*, 219. DOI: 10.1038/s41598-023-50660-w.

[38] Boutkbout, M. N. M.; EL Ouafya, H.; Halila, M.; Aamor, M.; Naciria, L.; Reda, C. M.; Ikena, W.; EL Ouafyb, T., Computational DFT Study on Donor and Spacer Substitution in Arylamine-Based Push-Pull Molecules for Enhanced Photovoltaic Performance, *Phys. Chem. Res.* **2025**, *13*,2, 197-215, DOI: 10.22036/pcr.2025.480570.2580.

[39] Chang-Guo, Z.; Jeffrey A. N.; David A. D., Ionization Potential, Electron Affinity, Electronegativity, Hardness, and Electron Excitation Energy: Molecular Properties from Density Functional Theory Orbital Energies, *J. Phys. Chem. A.* **2003**, *107*(20), 4184-4195, DOI: 10.1021/jp0225774.

[40] Vanasundari, K.; Balachandran, V.; Kavimani, M.; Narayana, B., Molecular docking, vibrational, structural, electronic and optical studies of {4-(2,6) dichlorophenyl amino 2-methylidene 4-oxobutanoic acid and 4-(2,5)} dichlorophenyl amino 2-methylidene 4-oxobutanoic acid – A comparative study. *J. Mol. Struct.*, **2018**, *1155*, 21-38, DOI: 10.1016/j.molstruc.2017.11.002.